Bioorg. Med. Chem. 28 (2020) 115794

Contents lists available at ScienceDirect

Bioorganic & Medicinal Chemistry

journal homepage: www.elsevier.com/locate/bmc

Optimization of kinetic stabilizers of tetrameric transthyretin: A prospective ligand efficiency-guided approach

Ellen Y. Cotrina [a], Daniel Blasi [b], Marta Vilà [c], Antoni Planas [c], Cele Abad-Zapatero [d], Nuria B. Centeno [e], Jordi Quintana [b,e], Gemma Arsequell [a,*]

[a] Unit of Glycoconjugate Chemistry, Institut de Química Avançada de Catalunya (IQAC−CSIC), Barcelona, Spain
[b] Drug Discovery Platform, Parc Científic de Barcelona, Barcelona, Spain
[c] Laboratory of Biochemistry, Institut Químic de Sarrià, Universitat Ramon Llull, Barcelona, Spain
[d] Center for Biomolecular Sciences, Chicago, IL, USA
[e] Research Group on Biomedical Informatics, Universitat Pompeu Fabra (UPF), Barcelona, Spain

ARTICLE INFO

Keywords:
Transthyretin
Iododiflunisal
TTR tetramer stabilizer
Inhibitors
Protein–ligand interactions
Ligand efficiency indices (LEI)
LEI-based approach
Drug discovery

ABSTRACT

In the past few years, attempts have been made to use decision criteria beyond Lipinski's guidelines (Rule of five) to guide drug discovery projects more effectively. Several variables and formulations have been proposed and investigated within the framework of multiparameter optimization methods to guide drug discovery. In this context, the combination of Ligand Efficiency Indices (LEI) has been predominantly used to map and monitor the drug discovery process in a retrospective fashion. Here we provide an example of the use of a novel application of the LEI methodology for prospective lead optimization by using the transthyretin (TTR) fibrillogenesis inhibitor iododiflunisal (IDIF) as example. Using this approach, a number of compounds with theoretical efficiencies higher than the reference compound IDIF were identified. From this group, ten compounds were selected, synthesized and biologically tested. Half of the compounds (**5**, **6**, **7**, **8** and **10**) showed potencies in terms of IC50 inhibition of TTR aggregation equal or higher than the lead compound. These optimized compounds mapped within the region of more efficient candidates in the corresponding experimental nBEI-NSEI plot, matching their position in the theoretical optimization plane that was used for the prediction. Due to their upstream (North-Eastern) position in the progression lines of NPOL = 3 or 4 of the nBEI-NSEI plot, three of them (**5**, **6** and **8**) are more interesting candidates than iododiflunisal because they have been optimized in the three crucial LEI variables of potency, size and polarity at the same time. This is the first example of the effectiveness of using the combined LEIs within the decision process to validate the application of the LEI formulation for the prospective optimization of lead compounds.

1. Introduction

Transthyretin (TTR) is a human tetrameric protein produced in the liver hepatocytes, choroid plexus and retina.[1,2] TTR is involved in the extracellular transport of thyroid hormones and vitamin A, through a complex with serum retinol-binding protein (RBP). The protein functions as backup transporter for thyroxine (T4) in plasma, and as a main transporter in cerebrospinal fluid. Interestingly, TTR has a neuroprotective role against Alzheimer's disease (AD).[3,4,5] Several mutations in the TTR sequence are the cause of a series of rare but serious amyloid diseases.[6] TTR tetrameric stabilization has been defined as the basis for one of the possible therapeutic strategies for the TTR-related

Abbreviations: H-β-Ala-OMe.HCl, β-alanine methyl ester; B_2Pin_2, Bis(pinacolato)diboron or 4,4,4′,4′,5,5,5′,5′-octamethyl-2,2′-bi-1,3,2-dioxaborolane; $B(OMe)_3$, Trimethyl borate; DCC, *N*,*N*′-dicyclohexylcarbodiimide, IPy_2BF_4, bis(pyridine)iodonium tetrafluoroborate; NCS, *N*-chlorosuccimide; DIPEA, *N*,*N*-diisopropylethylamine; DMSO, dimethylsulfoxide; EtAcO, ethyl acetate; HOBt, 1-hydroxybenzotriazol; HRMS, high-resolution mass spectrometry; HPLC, high performance liquid chromatography; ^{1}H NMR, proton nuclear magnetic resonance; rt, room temperature; RT, retention time; TBAI, Tetrabutyl ammonium iodide; $Pd(PPh_3)_4$, Tetrakis (triphenylphosphine)palladium(0); ^{t}BuONO, *tert*-butyl nitrite; ($Pd_2(dba)_3$), *Tris*(dibenzylideneacetone)dipalladium(0); XPhos, 2-Dicyclohexylphosphino-2′,4′,6′-triisopropylbiphenyl.

* Corresponding author at: Unit of Glycoconjugate Chemistry. Institut de Química Avançada de Catalunya (IQAC−CSIC), Jordi Girona-18-26, E08034 Barcelona, Spain.
E-mail address: gemma.arsequell@iqac.csic.es (G. Arsequell).

https://doi.org/10.1016/j.bmc.2020.115794
Received 13 August 2020; Received in revised form 23 September 2020; Accepted 24 September 2020
Available online 6 October 2020

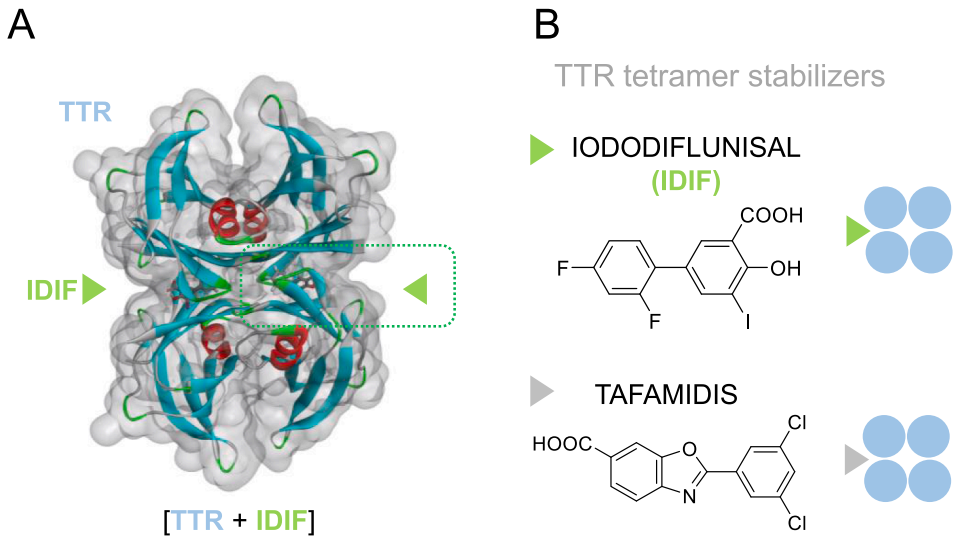

Fig. 1. a) Binary complex TTR with IDIF (PDB 1Y1D); B) Chemical structures of two TTR tetramer stabilizers, the small-molecule biphenyl compound Iododiflunisal (IDIF) and the benzoxazole drug Tafamidis, a registered drug for FAP.

amyloid diseases,[7,8,9] which include familial amyloid polyneuropathy (FAP),[10,11] familial amyloid cardiomyopathy (FAC),[12] senile systemic amyloidosis (SSA)[13] and central nervous system selective amyloidoses (CNSA).[14] Currently, the Protein data Bank[15] contains more than 300 crystallographic structures of TTR, most of them in complex with small molecule ligands.[16,17] Structurally diverse families of compounds are known to stabilize effectively TTR preventing its aggregation in vitro. [18,19] The orphan drug Tafamidis (Vyndaqel®), an small-molecule obtained by an structure-base design,[20] was the first drug to obtain approval for FAP treatment.[21] Another drug, Tolcapone, for the treatment of Parkinson's disease has been repositioned for FAP.[22] Additional TTR tetramer stabilizers are the small-molecule AG10 now in phase 3 trial (NCT03860935)[23] and the palindromic molecule mds84 in preclinical development.[24] Alternative therapeutic strategies are gene-silencing therapies, as the antisense oligonucleotide inotersen[25] and the small interfering RNA (siRNA) patisiran.[26]

One of our contributions to this ongoing drug discovery effort focused on TTR amyloid diseases has been the preclinical development of Iododiflunisal (IDIF, Figure 1).[27] Our lead compound is a iodinated derivative of the non-steroidal anti-inflammatory drug (NSAID) Diflunisal.[28] *In vitro* biochemical and biophysical evidences as well as *in vivo* animal studies support the interest on this lead.[29,30,31]

Since the seminal work of Lipinski and collaborators[32] there has been an extensive effort to optimize medicinal chemistry efficiency in order to reduce the high attrition rates of drug candidates.[33-35] A line of research is directed towards defining and using alternative variables, more aligned with drug efficacy that the target affinity alone, which has been the dominant parameter in medicinal chemistry for decades. These so called efficiency indices or composite parameters are metric-based rules and visualization tools to help in guiding medicinal chemists in the design of new compounds with more favorable properties.[36-39] An early example is Ligand Efficiency (LE)[40] suggested by Hopkins and collaborators[41] that proposed binding energy (ΔG) per heavy atoms as a metric for lead selection. This concept has given rise to an increasing range of ligand efficiency indices (LEIs) that combine potency or affinity with molecular weight (MW), polar surface area (PSA) and other ligand properties (Table 1).[42] Other indices such as ligand lipophilicity efficiency (LLE)[43,44] reflect the increased risk of high lipophilicity of drug candidates. A review of the application of ligand efficiency metrics related to size and

Table 1
Ligand efficiency indices names and definitions.

Index Name[a]	Definition
BEI	$p(K_i)$, $p(K_D)$ or $p(IC_{50})$/MW(kDA)
SEI	$p(K_i)$, $p(K_D)$ or $p(IC_{50})$/(PSA/100 Å^2)
NSEI	$p(K_i)$, $p(K_D)$ or $p(IC_{50})$; $-\log_{10}K_i$/(NPOL) = pK_i/NPOL (N + O)
NBEI	$P(K_i)$, $p(K_D)$, or $p(IC_{50})$; $-\log_{10}K_i$/(NHEAV) = pK_i/(NHEAV)
nBEI	$-\log_{10}(K_i/NHEAV)$; K_i, K_D, or IC_{50}
NHEAV	Number of heavy atoms (non-hydrogen in the compound)
NPOL	Number of polar atoms (N,O)
Efficiency plane[46]: NSEI, nBEI (x,y).	Lines of slope NPOL and intersect $\log_{10}$ NHEAV
Algebraic relationship[46] between nBEI, NSEI	Lines: nBEI = NPOL*NSEI + $\log_{10}$NHEAV

[a] Efficiency planes are defined as the combination of a polarity-based efficiency variable in the abscissa with a size-related variable in the ordinate. In these planes, polarity increases counter clockwise and in the NSEI, nBEI (x,y) planes, the slope of the lines increases by the number of polar atoms (NPOL = N + O) in the ligand. This quantity is equivalent to the number of hydrogen bond acceptors in the description of Lipinski's rule of 5. NPOL*NSEI stands for NPOL times NSEI; the slope of the lines is given by NPOL in the nBEI vs. NSEI plots.[46]

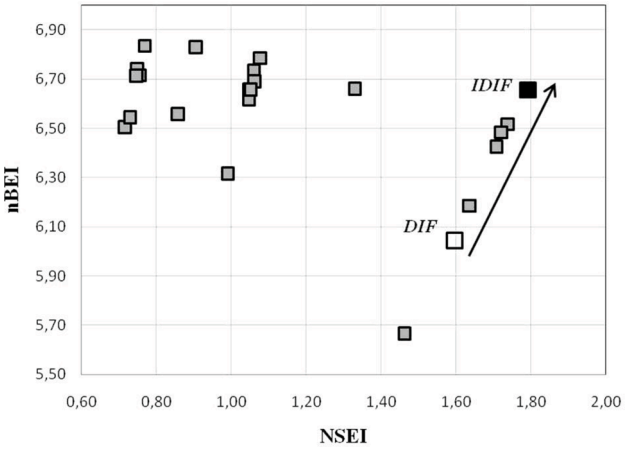

Fig. 2. Retrospective map of the Diflunisal/Iododiflunisal-based library: nBEI vs. NSEI plot shows that iododiflunisal (black square, IDIF), compared to diflunisal (white square, DIF), is the most effective TTR amyloid inhibitor for this chemical series, with optimized size and polarity parameters at the same time.

lipophilicity is provided in a previous publication by Hopkins et al.[45] A unified formulation of the LEIs, combining size and polarity in relation to a biological activity or affinity towards a biological target, has been presented in extensive detail.[46] In particular, it has been proposed that the combined variables NSEI-nBEI (x,y) (Table 1), can be used to map the chemico-biological space (CBS) to visualize trends across different targets and the progress of drug discovery and lead optimization projects. [39, 47-51] The uniqueness of this pair of variables [45] is that they provide an appealing two-dimensional, vector like, representation of the drug discovery process giving a sense of 'direction' and 'distance' in a Cartesian plane,[46,50] referred to as the 'Efficiency plane'. The formulation is such that the 'direction' (slope of the lines) is given by the number of polar atoms in the molecule (NPOL = N + O, equivalent to number of hydrogen-bond donors in the Lipinski Ro5), and the 'distance' (from the origin) is related to the affinity or biological activity of the compounds.[46] This graphical representation is very useful in distinguishing the direction (slope of the lines) of the optimization process (given by the scaffold atoms: NPOL and NHEAV defining the lines), from the potency gains (distance from the origin) that can be achieved with that chemical scaffold.

These combined size-polarity efficiency indices (nBEI-NSEI) have been applied in an "efficiency plane" to a series of proprietary biphenyl compounds with TTR aggregation inhibitory properties, in a retrospective fashion, to monitor the optimization progress of our lead compound IDIF.[52] In a further attempt to widen the applications of the LEIs formulation, an initial proof of the concept that the LEI metrics can be used in a prospective rather than a retrospective manner is presented in this work. Further work is encouraged to demonstrate conclusively the value of the LEIs formulation in lead optimization and preclinical candidate selection.

2. Results and discussion

Iododiflunisal optimization as a ground test. In an initial traditional optimization study of our lead compound IDIF, we examined the influence of small structural changes in the functional groups on the salicylic ring while leaving the 2,4-difluorophenyl core of the compound unchanged.[27] Using parallel synthesis methods, a biologically annotated library of 46 analogs was obtained after testing their activity. Only three iodinated compounds of the library were more potent (in terms of IC_{50} values) than iododiflunisal (IDIF) (SI Table S1). However, when these results were plotted in a nBEI (parameter relating the potency to the number of heavy atoms of the ligand) versus NSEI (parameter relating the potency to the number of polar atoms of the ligand) Cartesian plane (Figure 2), it emerged that the most efficient compound of the series i.e. the one with optimal size and polarity parameters at the same time, was still IDIF. As Figure 2 shows, several analogs with increasing efficiencies are found between diflunisal and IDIF along the NPOL = 3 slope but none is superior to it.

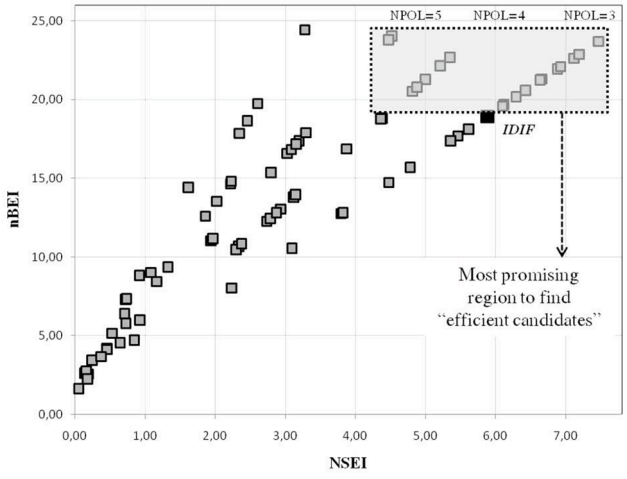

Fig. 3. nBEI vs. NSEI plot of the 80 selected docked compounds. Region highlighted shows compounds with increased efficiency (the reference compound IDIF is indicated by a black square). The direction(s) for the optimization path(s) for the different scaffolds containing NPOL values of 3, 4, 5 are indicated. The compounds with the largest NSEI, nBEI values in the North-East quadrant have combined optimum values of the NSEI, nBEI and the estimated affinity constant Ki*. Compounds with lower number NPOL atoms (NPOL < 5 following Lipinski guidelines) have higher probability of favorable permeability.

Virtual iododiflunisal optimization guided by a LEI prospective approach. In search of more efficient IDIF analogs, a three steps workflow methodology has been developed.[52] First, a IDIF scaffold-based search was effected on the MMsINC database[53] which allowed to extract 2300 virtual and commercial biphenyl compounds. Next, using an IDIF pharmacophore deduced from the crystallographic information of the complex TTR:IDIF,[29] this 2300 database was further filtered to a set of 1200 compounds that share the same IDIF interaction pattern with TTR. Lastly, these molecules were docked to a protein model from the IDIF:TTR X-ray crystal structure (PDB ID 1Y1D) and 80 of them were selected by their docking score value. Taking into account that the docking scores resulting from the docking calculations, using the MOE software package,[54] are an estimate of the binding free energy (herein ΔG*), it is possible to establish a relationship between K_i* (pseudo Ki) and ΔG*, through the equation: $\Delta G^* = -RT\ln K_i^*$. Following this approximation, K_i* values were estimated relating the docking score obtained from each best pose of the 80 selected molecules, which share the same biphenyl scaffold, and have a high similarity to IDIF and among themselves, to the free binding energy. In order to normalize these values, the experimental TTR binding K_i for IDIF obtained through an isothermal calorimetry experiment (ITC) was used (see Table S2 of S. I.).[31]

After this step, the results were plotted in a nBEI-NSEI plane.[52] The nBEI and NSEI parameters were calculated based on the estimation of their Ki*, with reference to the experimental Ki for IDIF. Figure 3 shows that compounds with efficiencies higher than IDIF can be found on the slope lines with NPOL = 3, 4 and 5.

To provide experimental validation of the virtual predictions on improved efficiency described above, a subset of compounds located at the region with theoretically more efficient candidates were selected, synthesized and subsequently tested for biological activity, and their experimental and theoretical efficiencies compared.

Synthesis of the selected compounds. Using criteria like minimal change on the structure, small changes in the number of polar atoms (NPOL) and ready synthesis, ten of the theoretically more efficient compounds were selected as test compounds. The structures of this subset of compounds (**1**–**10**) are depicted in Figure 4. Also, some of the corresponding non-halogenated derivatives of compounds **1**–**7**, in the position 5 of the biphenyl moiety (**1A**, **2A**, **4A**, **6A**, and **7A**), were included in the synthesis plan to compare the effects of the presence or absence of this particular halogen on the biological activity and hence the experimental efficiency of these molecules.

The general synthesis scheme of the compound series is outlined in Scheme 1. Biphenyl analogues (5-aryl salicylic derivatives) (**1A**, **2A**, **4A** and **6A**) were prepared by Suzuki cross-coupling reactions (SI, Figure S5).[55]

The iodinated biphenyl derivatives (**1**, **2**, **4**, **6**, **7**) were prepared from their parent compounds (**1A**, **2A**, **4A** and **6A**) by electrophilic aromatic iodination reaction using the iodinating reagent IPy_2BF_4 (Barluenga's reagent) in CH_2Cl_2 at room temperature.[56] Brominated derivatives (**3** and **5**) were prepared by electrophilic bromination using a mixture of potassium bromide and *N*-chlorosuccinimide (NCS) at room temperature. The synthesis of the polyhalogenated compound **7A** was initially designed as the previous analogs, involving a Suzuki coupling reaction between 5-iodosalicylic acid (**11**) and a polyhalogenated boronic acid.

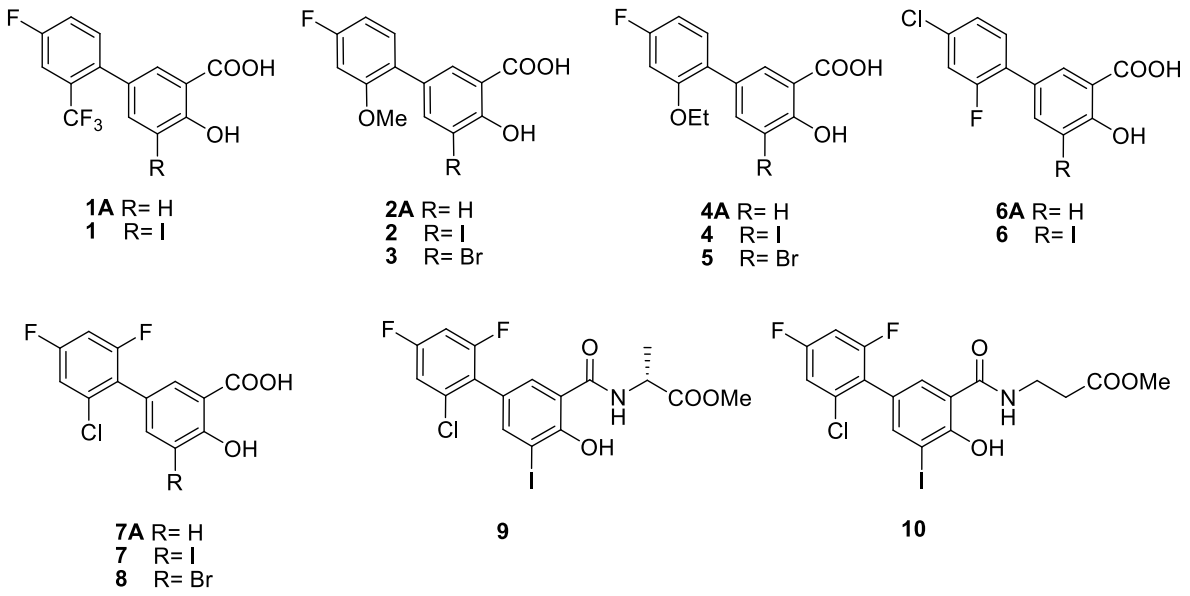

Fig. 4. Iododiflunisal analogs selected as theoretically more efficient than Iododiflunisal in terms of ligand efficiency parameters. (Some non-halogenated derivatives in the position 3 of the salicylic moiety are also shown).

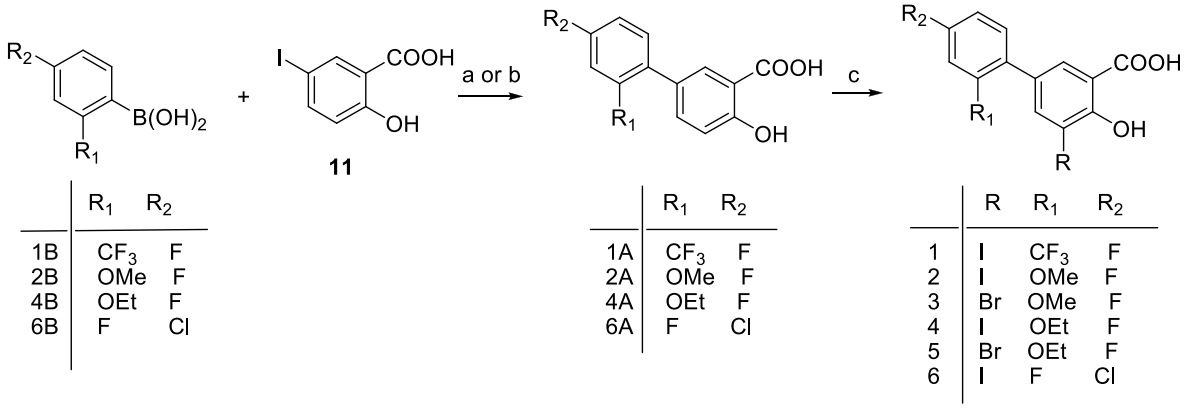

Scheme 1. Synthesis of Diflunisal and IDIF analogs. [a]Reagents and conditions: Suzuki-Miyaura cross-coupling reaction (Condition A: in water): a) aryl boronic acid (1 equiv.); 5-iodosalicylic acid (**11**) (1 equiv.), $Pd(OAc)_2$ (1 mol%), Na_2CO_3 (3 equiv.), H_20 (degassed water), rt, 3 h.; b) Suzuki-Miyaura cross-coupling reaction aryl boronic acid (1 equiv.), 5-iodosalicylic acid (**11**) (1 equiv.), $[Pd(PPh_3)_4]$ (1 mol%), Na_2CO_3 (3 equiv.), dioxane/water (4:1), 80 °C; c) for iodinated derivatives: IPy_2BF_4 (Barluenga's reagent) (1.5 equiv.), dichloromethane, rt, 1 h; or d) for brominated derivatives: NCS (1 equiv.), KBr (1 equiv.), ethanol.

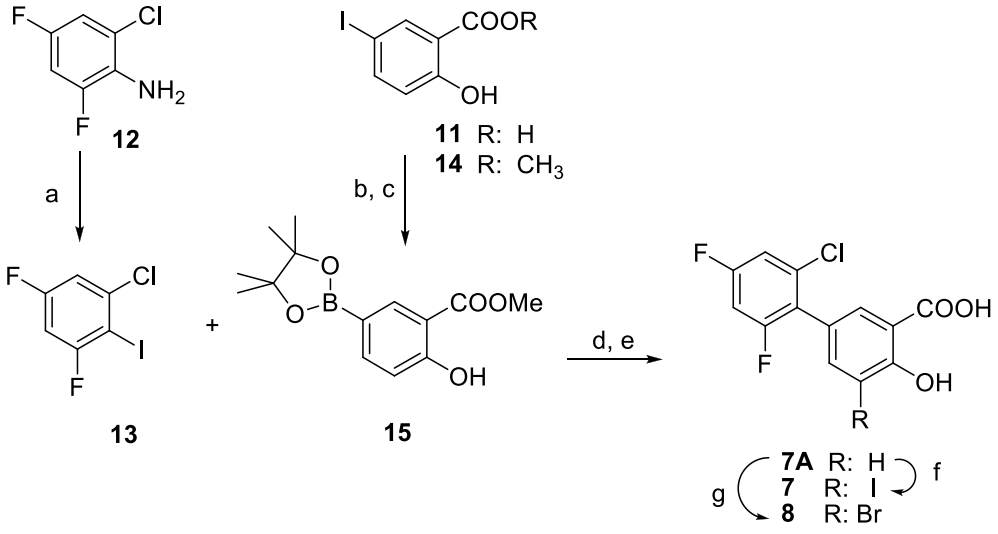

Scheme 2. Synthesis of polyhalogenated Diflunisal analogs. [a]Reagents and conditions: a) Tetrabutylammonium iodide (TBAI) (1.1 equiv.), CuI (1.1 equiv.), *tert*-butyl nitrite (^{t}BuONO) (3 equiv.), acetonitrile, 80 °C; b) 5-iodo salicylic acid (**11**), TMSCl (4 equiv.), MeOH, 110 °C, 24 h; c) methyl 5-iodosalicylate (**14**) (1 equiv.), bis(pinacolato)diboron (B_2Pin_2) (2 equiv.), $Pd_2(dba)_3$ (2 mol%), XPhos (4 mol%), KOAc (3 equiv.), dioxane, 110 °C; d) Suzuki-Miyaura coupling: boronate **15** (1 equiv.), iodinated compound **13** (1 equiv.), Na_2CO_3 (3 equiv.), $Pd(PPh_3)_4$ (5 mol%), dioxane, 110 °C; e) LiOH (4 equiv.), H_2O/dioxane, 80 °C, 30 min.; f) IPy_2BF_4 (Barluenga's reagent) (1.5 equiv.), CH_2Cl_2, rt, 1 h; g) NCS (1 equiv.), KBr (1 equiv.), ethanol.

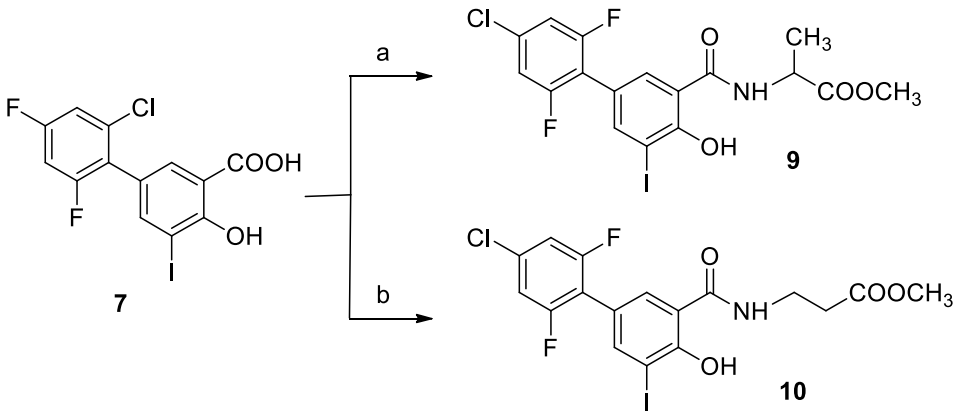

Scheme 3. Synthesis of iododiflunisal amino acid conjugated analogs. [a]Reagents and conditions: a) H-Ala-OMe.HCl (1 equiv.), DCC, HOBt, DIPEA, dichloromethane, rt, 50%; b) β-Ala-OMe.HCl (1 equiv.), DCC, HOBt, DIPEA, dichloromethane, rt, 77%.

Table 2
Inhibition of acid-induced fibrillogenesis by compounds under study: IC_{50} values measured by the kinetic turbidimetric assay[a] and the corresponding nBEI-NSEI indices values.[b]

Compound	X	IC_{50} (μM)	RA (%)	nBEI	NSEI
IDIF	I	4.2 ± 0.2	94.0 ± 0.5	6.66	1.79
1A	H	23.1 ± 4.3	60.4 ± 0.3	5.96	1.55
1	I	7.2 ± 0,1	87.0 ± 1.6	6.49	1.71
2A	H	6.0 ± 0.2	87.8 ± 0.9	6.50	1.31
2	I	5.3 ± 0.3	90.3 ± 1.3	6.58	1.32
3	Br	5.2 ± 0.5	95.5 ± 1.6	6.59	1.32
4A	H	6.1 ± 0.5	88.8 ± 0.3	6.52	1.30
4	I	5.1 ± 1.1	91.1 ± 0.7	6.61	1.32
5	Br	4.3 ± 0.4	89.9 ± 0.8	6.69	1.34
6A	H	21.7 ± 1.6	77.3 ± 4.9	5.92	1.55
6	I	3.9 ± 1.7	88.5 ± 1.4	6.69	1.80
7A	H	7.2 ± 0.5	89.1 ± 1.1	6.42	1.71
7	I	4.6 ± 0.2	91.0 ± 0.4	6.64	1.78
8	Br	3.6 ± 0.2	89.0 ± 2.2	6.74	1.81
9	I	6.0 ± 0.5	89.0 ± 0.6	6.64	1.04
10	I	3,7 ± 0.3	90.0 ± 0.1	6.85	1.09

[a] Kinetic turbidity assay: 0.4 mg/mL TTR-Y78F, 0–40 μM inhibitor, pH 4.2, 37 °C.
[b] nBEI and NSEI values have been calculated by using the definitions listed in Table 1 using the pIC_{50} value for the biological activity.

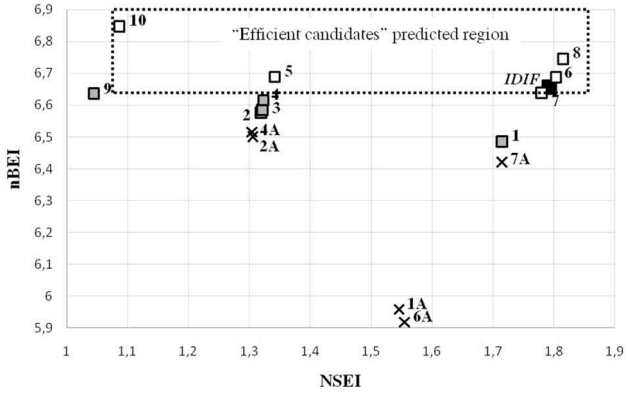

Fig. 5. nBEI vs. NSEI plot based on the experimental data (IC_{50} values) obtained from the kinetic turbidimetry assay. Black square corresponds to the reference compound IDIF; crosses are the non-halogenated derivatives for the corresponding compounds as indicated in Figure 4; compounds with a similar or higher efficiency compared with IDIF (in good agreement with the predictions performed in this study) are highlighted in the "Efficient candidates" region as white squares; grey squares are the compounds less efficient than IDIF (in which the prediction fails).

Polyhalogenated boronic acids are especially challenging coupling partners for Suzuki-Miyaura reactions because they quickly deboronate under basic conditions.[57,58]

Due to the inherent difficulties of these polyhalogenated boronic acids, an alternative pathway was designed based on a pinacol boronate ester (Scheme 2). Thus, a new pinacol boronate ester (**15**) was prepared. The Suzuki coupling reaction between the iodocompound **13** and the newly prepared boronate ester **15** was done in dioxane/water (9:1) at 80 °C catalyzed by *tetrakis*(triphenylphosphine)palladium (0) [Pd $(PPh_3)_4$] (5 mol%), in the presence of Na_2CO_3 as base providing the desired biphenyl compound **7A** (Scheme 2).

Amino acid conjugates **9** and **10** were prepared through a similar method as we have reported previously,[27] starting from biphenyl carboxylic acid derivative **7**, by a coupling reaction either with the methyl ester of L-alanine or the one from β-alanine, respectively (Scheme 3). In both reactions *N,N'*-dicyclohexyl carbodiimide (DCC) was used as the coupling reagent used in the presence of 1-hydroxybenzotriazol (HOBt) for the amide bond formation.[59]

Experimental validation of the efficiency. This set of 15 synthesized compounds and the reference IDIF, were tested in a turbidimetric in vitro assay to evaluate their potential activity as TTR fibril inhibitors.[60] The protocol uses a highly amyloidogenic TTR variant (Y78F) which enables kinetic monitoring of protein aggregation in short time under acid-induced fibrillogenesis conditions. One of the parameters that can be assessed through this method is the IC_{50} value, which is the concentration of inhibitor at which the initial rate of fibril formation is half than in the absence of inhibitor. A second parameter is the percentage of reduction in fibril formation rate (RA%) at high concentration of test compound relative to the rate obtained in the absence of compound. RA values of 100% indicate that the inhibitor can fully prevent the formation of fibrils. Experimental IC_{50} values are reported in Table 2, showing that compounds **5**, **6**, **7**, **8** and **10** have a similar or even higher fibrillogenesis inhibition activity compared to iododiflunisal.

Evaluation of the LEI predictive power. To evaluate the accuracy of the LEI predictions and the extend of the optimization of iododiflunisal in terms of efficiency gain, the experimental potencies of the compounds expressed as IC_{50} values have been used to calculate the corresponding experimental nBEI and NSEI values for each molecule (Table 2). The efficiency indices (NSEI, nBEI) for a biological assay can be calculated similarly using the IC_{50} listed in Table 2.[46] Also, to visualize the predictive power of this methodology, the predictive map shown in Figure 3, was redrawn as the experimental map presented in Figure 5. A rough 50% matching rate was found between predicted and experimental efficiencies of compounds with five clear failures in the case of compounds **1**, **2**, **3**, **4** and **9**. However, only product **1** is rather far apart from the region selected in the prediction step. On the other hand, although product **7** is at the border of this best candidates region, an

interesting fact is that no mismatches between the efficiency maps have occurred in case of compounds **5**, **6**, **8** and **10** which, in turn, are most potent than iododiflunisal.

Appearing above IDIF in the nBEI-NSEI map and on top of the progression line of NPOL = 3, product **8** is the most efficient candidate of this series. The potency of this compound (IC_{50} = 3.6 μM), compares with the most potent TTR amyloidogenic inhibitor known up to date, triiodophenol[61] (IC_{50} = 3.2 μM), and provides an approximate idea of the level of optimization achieved. This optimization capacity of the LEIs is reinforced when the comparison between the biological activities of **8** and Tafamidis, the drug marketed in Europe for the treatment of FAP, shows that product **8** has an enhanced potency and efficiency. Thus, under the kinetic turbidity assay conditions, Tafamidis presents an IC_{50} = 6.59 μM, and values of 6.48 and 1.30 for nBEI and NSEI respectively. Besides **8**, two more compounds, **6** (3.9 μM, NPOL = 3) and **5** (4.3 μM, NPOL = 4) have been identified and characterized as better and more efficient candidates than IDIF. The main feature of this triad (**5**, **6** and **8**) is that their three crucial LEI variables (potency, size and polarity) have been optimized at the same time.

Finally, it is worth noting that the non-halogenated derivatives at the position 5, that were also included among the test compounds, show lower potencies than their halogenated counterparts, and are found outside the preferred candidate efficiency region. A particular case is **6A** which shows a potency of 21.7 μM and a very poor efficiency behavior, far from its iodinated counterpart **6** (3.9 μM); this reinforces our hypothesis on the important role that halogen atoms play on TTR tetramer stabilization and prevention of fibril formation.

3. Conclusions

Here we presented the first experimental evidence of a novel application of the LEI formulation for prospective lead optimization by using the iododiflunisal chemico-biological space as example. The results also suggest that the LEI methodology, both retrospective and prospective, may be easily combined and integrated with computational workflows such as pharmacophore modeling and docking experiments. This prospective LEI approach has allowed us to identify a triad of compounds with optimized properties (potency, size and polarity) with respect to iododiflunisal. Significantly, compound **8** that maps in the extreme North-East corner of the efficiency plane, has the best combination of IC_{50} and physico-chemical properties (size, polarity) as 'combined' in the corresponding NSEI, nBEI values (Table 2). Compound **8** compares very favorably with triiodophenol (3.2 μM), one of the most potent TTR fibrillogenesis inhibitor known up to date, which may be of interest for future drug developments in the field of TTR-related amyloid diseases treatment. In contrast, compound **10** with better IC_{50} than IDIF and slightly larger values of efficiency per size (IC_{50} = 3.7 vs. 4.2; nBEI = 6.85 vs. 6.66, respectively) exhibits a significantly lower value of the polarity efficiency NSEI (NSEI = 1.09 vs. 1.79) (Table 2) making it significantly more polar and less suitable for further development.

3.1. Experimental section

3.1.1. Synthesis and characterization of compounds.

All diflunisal and IDIF analogues were prepared following the Schemes 1, 2 and 3. The synthesis and characterization are described in the SI.

Protein and inhibitors. The human TTR variant Y78F protein was recombinant expressed in *E. coli* and purified as already reported.[60] All assays were performed in buffers containing a final 5% (v/v) DMSO concentration for solubilization of the ligands.

Kinetic Turbidimetric Assay. Inhibition of fibrillogenesis was determined by the kinetic turbidimetric assay previously reported.[60] In seven different wells of a 96-well microplate, 20 μL of a 4 mg/mL TTR variant Y78F solution in 20 mM potassium phosphate buffer, 100 mM KCl, and 1 mM EDTA at pH 7.6, was mixed with an 80 μL solution of inhibitor prepared by mixing different volumes of a stock solution of the compound in H_2O/DMSO (1:1) to give a range of final compound concentrations of 0–40 μM. DMSO content was adjusted to a final 5% (v/v), where all ligands tested are soluble. After 30 min incubation at 37 °C with 15 s shaking every minute, 100 μL of 400 mM KAcO, 100 mM KCl, and 1 mM EDTA buffer at pH 4.2 were added to each well. The final mixture, containing 0.4 mg/mL TTR, 0 to 40 μM ligand, and 5% DMSO, was incubated at 37 °C with 15 s shaking every minute. Absorbance at 340 nm was monitored for 1.5 h at 1 min intervals. A control solution of the ligands at the highest concentration (40 μM) following the same procedure in the absence of TTR was also monitored, showing that the ligands remained soluble and no turbidity due to colloidal aggregation was observed. Initial rates of protein aggregation (ν_0) were obtained from the linear plot absorbance versus time. The dependence of ν_0 on inhibitor concentration is defined as:

$$\upsilon_0 = A + B \cdot e^{-C[I]}$$

where ν_0 is the initial rate of fibril formation (in absorbance units per hour, AU·h^{-1}) and [I] the concentration of the inhibitor (μM). From the adjustable parameters, the IC_{50} (inhibitor concentration at which the initial rate of protein aggregation is half than that in absence of inhibitor) and RA(%) (percentage reduction of amyloidosis at high inhibitor concentration) were calculated (See SI, Fig. S3)

Crystallographic Complex. 3D atomic coordinates of the TTR-iododiflunisal complex (PDB ID: 1Y1D)[29] used in the present work were obtained from the structural information available in the Protein Data Bank (PDB) (http://www.rcsb.org). Before the ligand–protein interactions mapping, a previous processing of the pdb file was needed. The asymmetric crystal unit of TTR complexes is formed by a dimer, two ligand molecules (one for each binding site) and water molecules; taking this into account, coordinates for the tetrameric form of TTR were obtained by applying the crystallographic symmetry transformations described in the pdb file. For residues with multiple conformations, we considered the one with the highest occupation factor.

Hydrogen Atoms Refinement. Added hydrogen atoms were energy-minimized by using the Protonate 3D package implemented in MOE 2013.08.[54] Ligand partial charges were obtained by computing the electrostatic-potentials around the optimized structures using MOE 2013.08. Minimization was carried out using a distance dependent dielectric constant and a cutoff distance of 10 Å for Van der Waals interactions. Hydrogen atoms refinement was accomplished using 1000 cycles of steepest descents followed by conjugate gradient until the maximum gradient of the energy was smaller than 0,05 kcal/mol·Å^2.

Data Set Selected. A set of 2300 biphenylic compounds was extracted from MMsINC Database.[53] LigX package (MOE 2013.08) was used for the hydrogen addition and ligand preparation.

Docking Experiments. MOE 2013.08 package was used to perform the docking studies of the data set selected with the crystallographic TTR complex. Alpha Triangle was used as placement method, Alpha HB as score function and MMF94 as forcefield in the refinement step of the docking solutions.

Author contributions

Overall research design and writing of the manuscript: G.A., C.A.Z., A.P., N.B.C., J.Q., D.B. Computational studies: D.B. Chemistry experiments: G.A. Biological experiments: E.Y.C., M.V.

Declaration of Competing Interest

The authors declare no competing financial interest.

Acknowledgements

We thank Dr. Lluís Bosch for help on the synthesis work. Funding

Sources. This work was supported by a Grant 080530/31/32 from the Fundació Marató de TV3, Barcelona, Spain (to G.A, A.P., and J.Q.) and a Grant from Plan Nacional, Ministerio de Economía y Competitividad (Ref: CTQ2010-20517-C02-02) to G.A.

Appendix A. Supplementary material

Supplementary data to this article can be found online at https://doi.org/10.1016/j.bmc.2020.115794.

References

1 Vieira M, Saraiva MJ. Transthyretin: a multifaceted protein. *Biomol Concepts.* 2014;5:45–54.
2 Hamilton JA, Benson MD. Transthyretin: a review from a structural perspective. *Cell. Mol. Life Sci.* 2001;58:1491–1521.
3 Gião T, Saavedra J, Cotrina E, et al. Undiscovered roles for transthyretin: from a transporter protein to a new therapeutic target for alzheimer's disease. *Int. J. Mol. Sci.* 2020;21:2075. https://doi.org/10.3390/ijms21062075.
4 Alemi M, Silva SC, Santana I, Cardoso I. Transthyretin stability is critical in assisting beta amyloid clearance – Relevance of transthyretin stabilization in Alzheimer 's disease. *CNS Neurosci. Ther.* 2017;23:605–619.
5 Cotrina EY, Gimeno A, Llop J, et al. Calorimetric studies of binary and ternary molecular interactions between transthyretin, Aβ peptides and small-molecule chaperones towards an alternative strategy for Alzheimer's Disease drug discovery. *J. Med. Chem.* 2020;63:3205–3214.
6 Rowczenio DM, Noor I, Gillmore JD, Lachmann HJ, Hawkins PN, Obici L, Westermark P, Grateau G, Wechalekar AD. Online registry for mutations in hereditary amyloidosis including nomenclature recommendations. *Hum. Mutat.* 2014;11. https://doi.org/10.1002/humu.2261, 35–E2403-E2412.
7 Nevone A, Merlini G, Nuvolone M. Treating protein misfolding diseases: therapeutic successes against systemic amyloidoses. *Front. Pharmacol.* 2020;11:1024. https://doi.org/10.3389/fphar.2020.01024.
8 Almeida MR, Gales L, Damas AM, Cardoso I, Saraiva MJ. Small transthyretin (TTR) ligands as possible therapeutic agents in TTR amyloidoses. *Curr. Drug Targets. CNS Neurol. Disord.* 2005;4:587–596.
9 Connelly S, Choi S, Johnson SM, Kelly JW, Wilson Ia. Structure-Based Design of Kinetic Stabilizers That Ameliorate the Transthyretin Amyloidoses. *Curr. Opin. Struct. Biol.* 2010;20:54–62.
10 Andrade C. A peculiar form of peripheral neuropathy. *Brain.* 1952;75:408–427.
11 Saraiva MJ, Magalhaes J, Ferreira N, Almeida MR. Transthyretin deposition in familial amyloidotic polyneuropathy. *Curr. Med. Chem.* 2012;19:2304–2311.
12 Griffin JM, Maurer MS. Transthyretin cardiac amyloidosis: A treatable form of heart failure with a preserved ejection fraction. *Trends Cardiovasc. Med.* 2019;S1050–1738(19):30166–30175.
13 Manso MC, Marques DP, Rocha SL, Rodeia SC, Domingos R. Senile systemic amyloidosis: an underdiagnosed disease. *Eur. J. Case Rep. Intern. Med.* 2017;4, 000725. https://doi.org/10.12890/2017_000725.
14 Sekijima Y, Hammarstrom P, Matsumura M, et al. Energetic characteristics of the new transthyretin variant A25T may explain its atypical central nervous system pathology. *Lab. Invest.* 2003;83:409–417.
15 Berman HM, Westbrook J, Feng Z, et al. The protein data bank. *Nucleic Acids Res.* 2000;28:235–242.
16 Palaninathan SK. Nearly 200 X-ray crystal structures of transthyretin: what do they tell us about this protein and the design of drugs for TTR amyloidoses? *Curr. Med. Chem.* 2012;19:2324–2342.
17 Nencetti S, Orlandini E. TTR fibril formation inhibitors: is there a SAR? *Curr. Med. Chem.* 2012;19:2356–2379.
18 Guo X, Liu Z, Zheng Y, et al. Review on the structures and activities of transthyretin amyloidogenesis inhibitors. *Drug Des. Devel. Ther.* 2020;14:1057–1081.
19 Ciccone L, Tonali N, Nencetti S, Orlandini E. Natural compounds as inhibitors of transthyretin amyloidosis and neuroprotective agents: analysis of structural data for future drug design. *J. Enzyme Inhib. Med. Chem.* 2020;35:1145–1162.
20 Bulawa CE, Connelly S, Devit M, et al. Tafamidis, a potent and selective transthyretin kinetic stabilizer that inhibits the amyloid cascade. *Proc. Natl. Acad. Sci. U.S.A.* 2012;109:9629–9634.
21 Coelho T, Maia LF, Martins da Silva A, et al. Tafamidis for transthyretin familial amyloid polyneuropathy: a randomized, controlled trial. *Neurology.* 2012;79:785–792.
22 Gámez J, Salvadó M, Reig N, et al. Transthyretin stabilization activity of the catechol-*O*-methyltransferase inhibitor tolcapone (SOM0226) in hereditary ATTR amyloidosis patients and asymptomatic carriers: proof-of-concept study. *Amyloid.* 2019;26:74–84.
23 Fox JC, Hellawell JL, Rao S, et al. First-in-human study of AG10, a novel, oral, specific, selective, and potent transthyretin stabilizer for the treatment of transthyretin amyloidosis: a phase 1 safety, tolerability, pharmacokinetic, and pharmacodynamic study in healthy adult volunteers. *Clin. Pharmacol. Drug Dev.* 2020;9:115–129.
24 Corazza A, Verona G, Waudby CA, et al. Binding of monovalent and bivalent ligands by transthyretin causes different short- and long-distance conformational changes. *J. Med. Chem.* 2019;62:8274–8283.
25 Benson MD, Waddington-Cruz M, Berk JL, et al. Inotersen treatment for patients with hereditary transthyretin amyloidosis. *N. Engl. J. Med.* 2018;379:22–31.
26 Adams D, Gonzalez-Duarte A, O'Riordan WD, et al. Patisiran, an RNAi therapeutic, for hereditary transthyretin amyloidosis. *N. Engl. J. Med.* 2018;379:11–21.
27 Mairal T, Nieto J, Pinto M, et al. Iodine atoms: a new molecular feature for the design of potent transthyretin fibrillogenesis inhibitors. *PLoS ONE.* 2009;4, e4124.
28 Berk JL, Suhr OB, Obici L, et al. Repurposing diflunisal for familial amyloid polyneuropathy: a randomized clinical trial. *JAMA.* 2013;310:2658–2667.
29 Gales L, Macedo-Ribeiro S, Arsequell G, Valencia G, Saraiva MJ, Damas AM. Human transthyretin in complex with iododiflunisal: structural features associated with a potent amyloid inhibitor. *Biochem. J.* 2005;388:615–621.
30 Ribeiro C, Oliveira SM, Guido LF, et al. Transthyretin stabilization by iododiflunisal promotes amyloid-β peptide clearance, decreases its deposition, and ameliorates cognitive deficits in an alzheimer's disease mouse model. *J. Alzheimers. Dis.* 2014;39:357–370.
31 Cotrina EY, Pinto M, Bosch L, et al. Modulation of the fibrillogenesis inhibition properties of two transthyretin ligands by halogenation. *J. Med. Chem.* 2013;56:9110–9121.
32 Lipinski CA, Lombardo F, Dominy BW, Feeney PJ. Experimental and computational approaches to estimate solubility and permeability in drug discovery and development settings. *Adv. Drug Deliv. Rev.* 2001;46:3–26.
33 Kola I, Landis J. Can the pharmaceutical industry reduce attrition rates? *Nat. Rev. Drug Discov.* 2004;3:711–715.
34 Waring MJ, Arrowsmith J, Leach AR, et al. An analysis of the attrition of drug candidates from four major pharmaceutical companies. *Nat. Rev. Drug Discov.* 2015;14:475–486. https://doi.org/10.1038/nrd4609.
35 Hinkson IV, Madej B, Stahlberg EA. Accelerating Therapeutics for Opportunities in Medicine: A Paradigm Shift in Drug Discovery. *Front Pharmacol.* 2020;11:770. https://doi.org/10.3389/fphar.2020.00770. Published 2020 Jun 30.
36 Segall M. Can we really do computer-aided drug design? *J. Comput. Aided. Mol. Des.*. 2011:121–124.
37 Segall M. Advances in multiparameter optimization methods for de novo drug design. *Expert Opin. Drug Discov.* 2014;9:803–817.
38 Yusof I, Shah F, Hashimoto T, Segall MD, Greene N. Finding the rules for successful drug optimisation. *Drug Discov. Today.* 2014;19:680–687.
39 Abad-Zapatero C, Champness EJ, Segall MD. Alternative variables in drug discovery: promises and challenges. *Future Med. Chem.* 2014;6:577–593.
40 Kuntz ID, Chen K, Sharp Ka, Kollman Pa. The Maximal Affinity of Ligands. *Proc. Natl. Acad. Sci. U. S. A.* 1999;96:9997–10002.
41 Hopkins AL, Groom CR, Alex A. Ligand efficiency: a useful metric for lead selection. *Drug Discov. Today.* 2004;9:430–431.
42 Abad-Zapatero C. Ligand efficiency indices for effective drug discovery. *Expert Opin. Drug Discov.* 2007;2:469–488.
43 García-Sosa AT, Hetényi C, Maran U. Drug efficiency indices for improvement of molecular docking scoring functions. *J. Comput. Chem.* 2009;31:174–184.
44 Shultz MD. Setting expectations in molecular optimizations: strengths and limitations of commonly used composite parameters. *Bioorg. Med. Chem. Lett.* 2013;23:5980–5991.
45 Hopkins AL, Keserü GM, Leeson PD, Rees DC, Reynolds CH. The role of ligand efficiency metrics in drug discovery. *Nat. Rev. Drug Discov.* 2014;13:105–121.
46 Abad-Zapatero C. *Ligand efficiency indices for drug discovery: towards an atlas-guided paradigm, Oxford*. UK: Academic Press, an imprint of Elsevier; 2013.
47 de Souza Neto LR, Moreira-Filho JT, Neves BJ, et al. Jr. *In silico* strategies to support fragment-to-lead optimization in drug discovery. *Front Chem.* 2020;8:93. https://doi.org/10.3389/fchem.2020.00093.
48 Abad-Zapatero C, Metz JT. Ligand efficiency indices as guideposts for drug discovery. *Drug Discov. Today.* 2005;10:464–469.
49 Abad-Zapatero C, Blasi D. Ligand efficiency indices (LEIs): more than a simple efficiency yardstick. *Mol. Inform.* 2011;30:122–132.
50 Christmann-Franck S, Cravo D, Abad-Zapatero C. Time-trajectories in efficiency maps as effective guides for drug discovery efforts. *Mol. Inform.* 2011;30:144.
51 Sugaya N. Ligand efficiency-based support vector regression models for predicting bioactivities of ligands to drug target proteins. *J. Chem. Inf. Model.* 2014;54:2751–2763.
52 Blasi D, Arsequell G, Valencia G, et al. Retrospective mapping of SAR data for TTR protein in chemico-biological space using ligand efficiency indices as a guide to drug discovery strategies. *Mol. Inform.* 2011;30:161–167.
53 Masciocchi J, Frau G, Fanton M, et al. MMsINC: a large-scale chemoinformatics database. *Nucleic Acids Res.* 2009;37:284–290.
54 Molecular Operating Environment (MOE), 2013.08; Chemical Computing Group Inc., 1010 Sherbooke St. West, Suite #910, Montreal, QC, Canada, H3A 2R7, 2013.
55 Suzuki A. Cross-coupling reactions of organoboranes: an easy way to construct C-C bonds (nobel lecture). *Angew. Chem. Int. Ed. Engl.* 2011;50:6722–6737.
56 Barluenga J. Recent advances in selective organic synthesis mediated by transition metal complexes. *Pure Appl. Chem.* 1999;71:1385–1391.
57 Kinzel T, Zhang Y, Buchwald SL. A new palladium precatalyst allows for the fast suzuki−miyaura coupling reactions of unstable polyfluorophenyl and 2-heteroaryl boronic acids. *J. Am. Chem. Soc.* 2010;132:14073–14075.
58 Robbins DW, Hartwig JF. A C-H borylation approach to Suzuki-Miyaura coupling of typically unstable 2-heteroaryl and polyfluorophenyl boronates. *Org. Lett.* 2012;14:4266–4269.

59 Sheehan JC, Hess GP. A new method of forming peptide bonds. *J. Am. Chem. Soc.* 1955;77:1067–1068.
60 Dolado I, Nieto J, Saraiva MJM, Arsequell G, Valencia G, Planas A. Kinetic assay for high-throughput screening of in vitro transthyretin amyloid fibrillogenesis inhibitors. *J. Comb. Chem.* 2005;7:246–252.
61 Miroy GJ, Lai Z, Lashuel HA, Peterson SA, Strang C, Kelly JW. Inhibiting transthyretin amyloid fibril formation via protein stabilization. *Proc. Natl. Acad. Sci. U.S.A.* 1996;93:15051–15056.